JOURNAL OF MOLECULAR ELECTRONICS VOL 6 155–166 (1990)

Extended Electron States in Proteins*

N. K. Balabaev, V. D. Lakhno and A. M. Molchanov
Research Computing Centre, USSR Academy of Science, Pushchino, Moscow Region, 142292, USSR

B. P. Atanasov
Central Laboratory of Biophysics, Bulgarian Academy of Science, Sofia 1113, Bulgaria

A new approach to the problem of electron states in the protein molecule is described. A 'dielectric cavity' model for a protein globule is used as a basis to consider the extended states which are mostly formed by the polarization field of the protein macromolecule. In a protein solution the size of such a state can be compared with the size of the macromolecule. The share of the extended states in the biomolecular processes of charge transfer is discussed. Electron energies of the ground and the first excited self-consistent states are calculated. Typical values of the predicted energies of absorption bands and luminescence are found to be *ca* 1000 nm for the ground state absorption band and *ca* 2000 nm for the excited state luminescence. Various ways of experimentally observing such states are discussed.

Keywords: Polaron; electron transfer; dielectric cavity

INTRODUCTION

The large-distance electron transfer is one of the central problems of molecular biology. It is a well established fact that the electron can move large distances in biological systems. Theoretical studies in this field were stimulated by de Vault and Chance,[1] who measured the temperature dependence of the rate of electron transfer from cytochrome c to chlorophyll. Currently, the predominant point of view considers this multi-tunnelling transport with an unambiguously identifiable intermediate to be one of the possible mechanisms of this phenomenon.[2,3] In application to biological systems, the theoretical foundations of electron transfer are due to Foerster,[4,5] Marcus,[6] Jortner[7] and Hopfield,[8,9] who in turn proceeded from the idea of non-radiatory electron transfer in condensed media, which was first suggested by Pekar[10] and Huang and Rhys.[11] The idea of polaron states in condensed media is the basic one for the theory of non-radiative electron transfer, and allows a deep insight into the processes of electron transfer in biological systems. Therefore, research into the theory of the polaron in condensed systems may significantly broaden our knowledge of the electron states and transfer in biological systems.

The most general representation of the polaron may be given by the picture of an electron which, if placed in a polar medium, goes to a self-localized state where it does not form chemical bonds with the atoms of the medium. The polaron may be imagined as an electron being trapped by a potential well formed by electron-induced polarization of the surrounding molecules of the medium.[10] Using this representation, it was discovered that there are multiple, not just one, discrete polaron states which have their own

*Presented at the Second International Symposium on Molecular Electronics and Biocomputers, Moscow, 11–18 September 1989.

0748-7991/90/030155-12 $06.00

Received 23 October 1989
Revised 22 March 1990

potential wells consistent with the electrons trapped.[12,13] One of the principal consequences is that even the first excited self-consistent polaron state has a large excitation region, and may include *ca* 10^3–10^4 or more molecules of the medium for water, ammonia and other polar liquids. These findings in turn point to the necessity for critically analysing the problem of large-distance electron transfers, namely their biological role and impact. This paper is concerned with studies of these states in protein macromolecules. We shall show that the allowance for the electron large-radius states may lead to many new results. The very fact that they exist suggests new types of absorption and luminescence in solutions of globular proteins. For a spherically symmetrical protein with an electron acceptor in the centre of the globule, the presence of an excited polaron state of large radius implies isotropy of binary chemical reactions under excitation.

This paper is intended to make the physical representation of the polaron in a condensed medium in agreement with the representation of the polaron properties of the protein molecule. We shall formulate simple mathematical models of the polaron states in the protein and discuss some of the effects to which they lead.

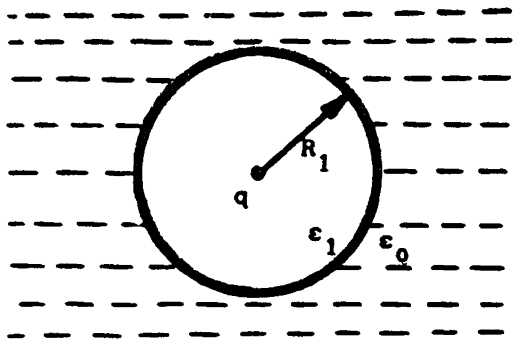

Figure 1. A two layer model of the protein globule.

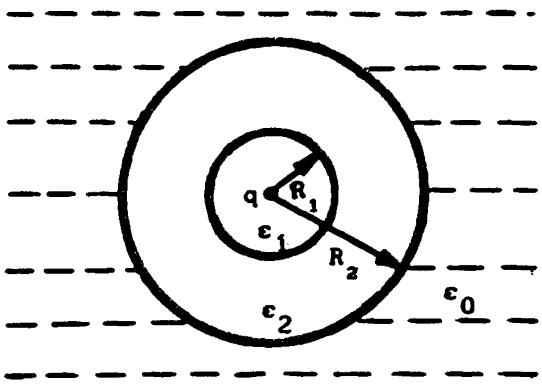

Figure 2. A three-layer model of the protein globule.

A CONTINUUM MODEL

To introduce what is meant by large-radius electron states in globular protein macromolecules it is necessary to examine continuum representations of these objects. It is also desirable to discuss the hierarchy of the continuum models that we shall use. The representation of a protein macromolecule that takes the form of a sphere in solution as its microphase was introduced by Bresler and Talmud,[14] who proceeded from hydrophobic properties of the protein. Progress in the modelling of protein globules led, in turn, to a whole set of electrostatic models.[15,16] The simplest of them, which is the model of dielectric cavity, is shown in Fig. 1. The model assumes that $\varepsilon_1 < \varepsilon_0$, which corresponds to a low static dielectric permittivity of the protein medium compared with the strongly polarized solvent. We stress that this model, although very simple, can give a qualitative explanation of many experimental findings on protein transport and electrophoresis.[17]

A more realistic model of a three-layer globule is shown in Fig. 2. This model allows for the contribution of different factors to dielectric permittivity in the region $R_1 < r < R_2$. The factors are the presence of amino acids residues, the penetration of water molecules into the superficial layer, the non-smoothness of the protein surface, etc. We assume that the solvent molecules cannot penetrate into the region $r < R_1$. In this model $\varepsilon_1 < \varepsilon_2 < \varepsilon_0$. Physical values of dielectric permittivities can be taken from an experiment: $\varepsilon_1 \approx 4$ is the value for *N*, *N*-dimethylacetamide, which is the monomeric analogue of the protein peptide framework (the solvent impervious region $r < R_1$); $\varepsilon_0 = 80$ is the value for water as a solvent; and the layer $R_1 < r < R_2$ is ascribed a mean value of $\varepsilon_2 \approx 40$, which in a more general sense is a parameter of the model. There are many models which assume that dielectric permittivity inside the globule depends on a coordinate (such as $\varepsilon = |\mathbf{r}|$),[18] and various non-local continuum models of dielectric cavities.[19]

While substantiating a mathematical model of polaron-type electron states in the protein globule, the ratio $\langle r \rangle / \bar{a}$ is the most important parameter, where $\bar{a}$ is the mean distance between two

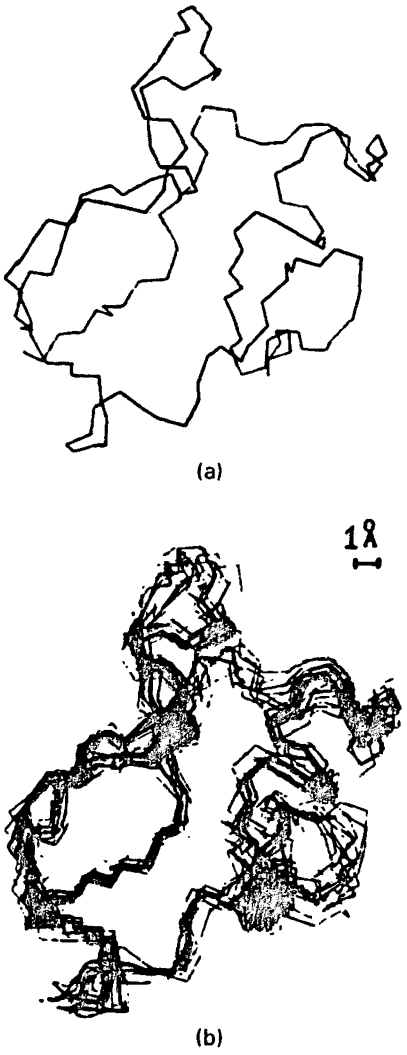

Figure 3. (a) A plane projection of the instantaneous configuration of the main chain $(-N-C^{\alpha}-C-)_{54}$ of a ferredoxin molecule and (b) overlapped projections for ten consecutive configurations of this molecule taken with a time Δt of 0.6 ps.

neighbouring atoms of the protein molecule and $\langle r \rangle$ is the effective polaron radius. The estimate $\bar{a}$ draws a clear distinction between a protein macromolecule and an ionic crystal for which the criterion $\langle r \rangle / \bar{a} \gg 1$ shows that the model is a continuum. In the ionic crystal polarization is caused by a small deviation of ions from their equilibrium states, so that $\bar{a} \approx a$, where a is the lattice constant. The protein molecule requires an additional averaging if the lifetime of the electron state is much larger than the characteristic time for oscillation of twisting degrees of freedom and for deviations of macromolecular polar groups, which normally is less than 10^{-12} s. This situation is illustrated in Fig. 3, which is the result of a molecular-dynamic computer simulation. In this way for the less long-lived states the model of a polar medium is 'more continuum' in the protein molecule than in the ionic crystal.

A POLARON MODEL FOR AN INFINITE ISOTROPIC MEDIUM (ACCORDING TO PEKAR[10])

A polaron description of the electron state in a polar medium usually starts with the assumption that the mean Coulomb field induced by the surplus elecron locally polarizes the medium. The electric field in turn influences the electron.[10] It is essential that the electron interacts only with the inertial part:

$$\mathbf{P}(\mathbf{r}) = \mathbf{P}_0(\mathbf{r}) - \mathbf{P}_\infty(\mathbf{r}) \tag{1}$$

where

$$\mathbf{P}_0 = \frac{\varepsilon_0 - 1}{4\pi\varepsilon_0}\,\mathbf{D},\quad \mathbf{P}_\infty = \frac{\varepsilon_\infty - 1}{4\pi\varepsilon_\infty}\,\mathbf{D}$$

are dipole moment densities of static and high-frequency polarizations, ε_0 and ε_∞ are static and high-frequency dielectric permittivities, respectively, and $\mathbf{D}$ is electric induction. Hence,

$$\mathbf{P}(\mathbf{r}) = \frac{\mathbf{D}(\mathbf{r})}{4\pi\tilde{\varepsilon}} \tag{2}$$

$\tilde{\varepsilon}^{-1} = \varepsilon_\infty^{-1} - \varepsilon_0^{-1}$ is the effective dielectric permittivity. The vector of electric induction caused by the distributed electron charge with density, $e\,|\,\Psi(\mathbf{r})\,|^2$, is equal to

$$\mathbf{D}(\mathbf{r}) = e\int |\,\Psi(\mathbf{r}')\,|^2\,\frac{\mathbf{r}-\mathbf{r}'}{|\,\mathbf{r}-\mathbf{r}'\,|^3}\,d\mathbf{r}' \tag{3}$$

where $\Psi(\mathbf{r})$ is the wave function, which can be obtained from the solution of the Schrödinger equation:

$$\frac{\hbar^2}{2\mu}\,\Delta\Psi(\mathbf{r}) + e\Pi(\mathbf{r})\Psi(\mathbf{r}) + W\Psi(\mathbf{r}) = 0 \tag{4}$$

where W is the electron energy. The potential $\Pi(\mathbf{r})$, created by the electron-induced polarization $\nabla\Pi(\mathbf{r}) = 4\pi\mathbf{P}(\mathbf{r})$, can, using Eqns (2) and (3), be found from the Poisson equation:

$$\Delta\Pi(\mathbf{r}) + 4\pi\tilde{\varepsilon}^{-1}e\,|\,\Psi(\mathbf{r})\,|^2 = 0 \tag{5}$$

The system of non-linear differential equations (4) and (5) fully determines the state of an electron in an infinite polar medium. Pekar[10] used the

variational principle to find the ground state of Eqns (4) and (5). Balabaev and Lakhno[12] integrated them numerically and obtained solutions corresponding to the excited polaron states different from the ground state. The approach that we have given here will be used further to describe the polaron states in a protein globule.

THE POLARON EQUATION FOR A PROTEIN GLOBULE

Our mathematical model of polaron states in the protein globule described by the model of dielectric cavity is based on the following assumptions: (i) the globule is neutral and has zero effective surface net charge on the layer boundaries; (ii) the electron states in the globule are thought of as the acceptor's potential-bound polaron states; (iii) each layer is described by a separate isotropic model of a continuous polar medium, and the electron wave function and the potential are assumed to be smooth both within and on the boundaries of each layer; and (iv) all the other assumptions are identical with those adopted to describe the polaron states in polar media.[10]

For a spherically symmetrical case the above assumptions yield the following equations for the polaron in a protein globule:

$$\frac{\hbar^2}{2\mu}\left(\frac{1}{r^2}\cdot\frac{\mathrm{d}}{\mathrm{d}r}\cdot r^2\cdot\frac{\mathrm{d}}{\mathrm{d}r}\right)\Psi(r) + e[\Pi(r)+\Phi(r)]\Psi(r) + W\Psi(r) = 0 \quad (6)$$

$$\frac{1}{r^2}\cdot\frac{\mathrm{d}}{\mathrm{d}r}\cdot r^2\cdot\frac{\mathrm{d}}{\mathrm{d}r}\cdot\Pi(r) + \frac{4\pi e}{\tilde{\varepsilon}_i}\Psi^2(r) = 0 \quad (7)$$

$$R_{i-1} < r < R_i, \qquad i = 1, 2\ldots; R_0 \equiv 0$$

where $\Phi(r)$ is the potential of the acceptor:

$$\Phi(r) = \begin{cases} q/\varepsilon_1 r + c_1 & r < R_1 \\ q/\varepsilon_2 r & r > R_1 \end{cases} \quad (8)$$

for the two-layer model of the globule ($\varepsilon_2 = \varepsilon_0$) and

$$\Phi(r) = \begin{cases} q/\varepsilon_1 r + c_1' & r < R_1 \\ q/\varepsilon_2 r + c_2' & R_1 < r < R_2 \\ q/\varepsilon_3 r & r > R_2 \end{cases} \quad (9)$$

for the three-layer model of the globule ($\varepsilon_3 = \varepsilon_0$). The constant c_1, c_1' and c_2' are defined from the continuity of potential $\Phi(r)$ at the boundaries of globular layers, $\Pi(r)$ is the potential of electron-induced polarization, μ is the electron effective mass, $\tilde{\varepsilon}_i^{-1} = \varepsilon_\infty^{-1} - \varepsilon_i^{-1}$ are the effective dielectric constants of the ith layer and ε_∞ is the high-frequency dielectric constant, which we assume to be identical for all the layers.

The natural boundary conditions for Eqns. (6) and (7) follow from the condition that the wave function is bounded and continuous and that the potential is continuous on the boundaries of globular layers, so that

$$\Psi'(0) + \frac{\mu q e}{\varepsilon_1 \hbar^2}\Psi(0) = \Pi'(0) = 0, \quad \Psi(\infty) = \Pi(\infty) = 0$$

$$\Psi(R_i - 0) = \Psi(R_i + 0), \quad \Psi'(R_i - 0) = \Psi'(R_i + 0)$$
$$\Pi(R_i - 0) = \Pi(R_i + 0), \quad \tilde{\varepsilon}_i\Pi'(R_i - 0) = \tilde{\varepsilon}_{i-1}\Pi'(R_i + 0) \quad (10)$$

Equation (6) is the Schrödinger equation for the electron in the potential $-(\Pi + \Phi)$, which is given in a self-consistent way by Eqn (7). Therefore, the non-linear system of differential equations (6) and (7) with the boundary conditions (10) describes bound polaron states in the protein globule. Its solution determines the wave function of the electron state Ψ and the electron energy W, in addition to the total energy of the I_F, which is given by the function

$$I_F[\Psi, \Pi] = \frac{\hbar^2}{2\mu}\int (\nabla\Psi)^2\,\mathrm{d}\mathbf{r} - e\int \Psi^2(\Pi + \Phi)\,\mathrm{d}\mathbf{r} + \sum_i \frac{\tilde{\varepsilon}_i}{8\pi}\int_{\Omega_i} (\nabla\Pi)^2\,\mathrm{d}\mathbf{r} \quad (11)$$

The last term of Eqn. (11) is integrated over regions Ω_i, which correspond to the layers of the dielectric cavity model. We should stress that Eqns (6) and (7) may be given by an independent variation of the function (11) with respect to the wave function $\Psi(r)$ and the potential $\Pi(r)$ with the wave function normalized by $\int \Psi^2(\mathbf{r})\,\mathrm{d}r = 1$.

SOLUTIONS OF POLARON EQUATIONS. THE GROUND STATE

The system of Eqns (6) and (7) with the boundary conditions (10) can be integrated numerically. The details of the algorithm are described in the Appendix. The case of polar media homogenity (all $\varepsilon_i = \varepsilon_0$) suggests an F-centre problem as solved by Lakhno and Balabaev.[13] If one considers a many-layer model of a protein globule, the solution of Eqns (6) and (7) is analogous to the previous one. It will be shown in the Appendix that

the system has a discrete set of solutions which are the self-consistent states of the electron and the polarization of the globule and its surroundings. Figure 4(a) shows a node-free solution (zero mode) and Fig. 4(b) the solution with a node which corresponds to the excited self-consistent state (first mode). In this section we consider only the findings for the ground state.

For the two- and three-layer models of a dielectric cavity, Table 1 lists the following values which characterize the self-consistent ground state: electron (W_{1S}) and total (I_{1S}) energies; electron levels (non-self-consistent) in 2S (W_{2S}) and in 2P (W_{2P}) states and the corresponding total energies (I_{2S}, I_{2P}), as well as the radii of the states ($\langle r\rangle_{1S}$, $\langle r\rangle_{2S}$, $\langle r\rangle_{2P}$) for both the models.

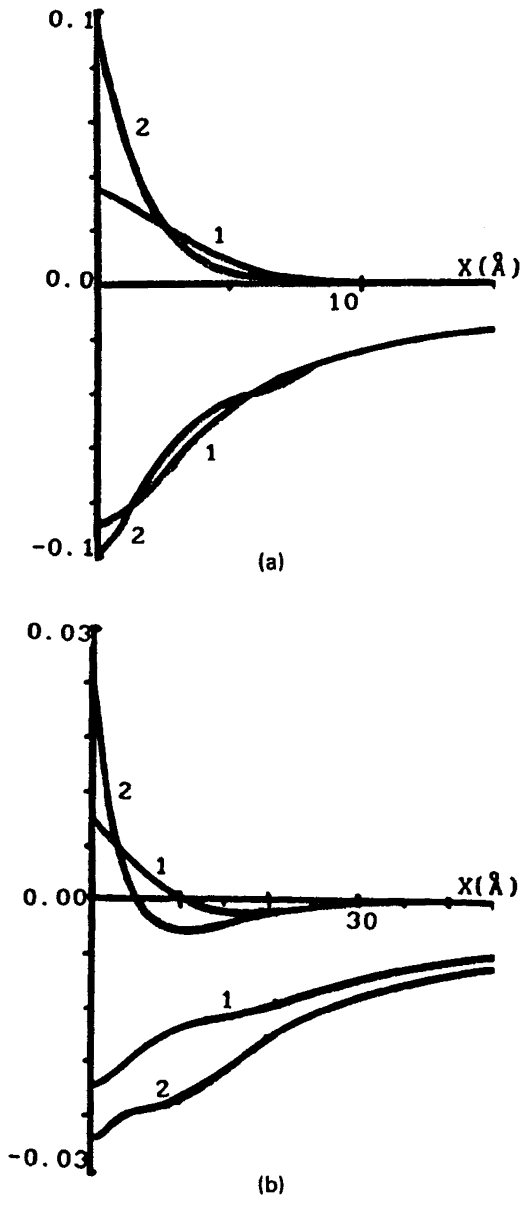

Figure 4. Solutions of the polaron equations for (1) the two-layer and (2) the three-layer models of the protein globule: (a) zero mode; (b) first mode. The upper part of the figure shows functions $\Psi(X)$ ($\int 4\pi X^2\Psi^2\, dX = 1$) and the lower part shows functions $\Pi(X)$ $\hbar^2/\mu e^3$ [$\approx 0.09\Pi(X)$].

Table 1. Polaron state characteristics in the protein globule

Physical value[a]	Two-layer model[b]		Three-layer model[c]	
	0-mode	1-mode	0-mode	1-mode
W_{1S}	−1.316	−0.401	−2.200	−1.035
W_{2S}	−0.529	−0.256	−0.697	−0.424
W_{2P}	−0.695	−0.283	−0.806	−0.413
I_{1S}	−0.508	−0.238	−1.243	−0.779
I_{2S}	0.280	−0.093	0.255	−0.169
I_{2P}	0.114	−0.120	0.146	−0.158
$\langle r\rangle_{1S}$	3.7	8.3	2.3	3.1
$\langle r\rangle_{2S}$	10.0	19.5	7.6	12.2
$\langle r\rangle_{2P}$	6.8	16.0	5.7	11.0

[a] The values of energies W_{1S}, W_{2S}, W_{2P}, W_{2P} and I_{1S}, I_{2S}, I_{2P} are in eV; the average radii $\langle r\rangle_{1S}$, $\langle r\rangle_{2S}$, $\langle r\rangle_{2P}$ are in Å.
[b] $\varepsilon_1 = 20$, $\varepsilon_2 = 80$, $\varepsilon_\infty = 2$, $R_1 = 15$ Å, $\mu = m_0$, $Z = 1$.
[c] $\varepsilon_1 = 4$, $\varepsilon_2 = 40$, $\varepsilon_3 = 80$, $\varepsilon_\infty = 2$, $R_1 = 7$ Å, $R_2 = 15$ Å, $\mu = m_0$, $Z = 1$.

It can be seen that for the more realistic three-layer model the polaron radius in the ground state is $\langle r\rangle_{1S} = 2.3$ Å, which is outside the approximation of the continuum model. Accordingly, the quantity $\Delta W_{1S,2P} = |W_{2P} - W_{1S}| \approx 1.2$ eV (*ca* 1000 nm) falls just inside the region of transitions with charge transfers of metal-containing proteins.[20,21]

THE EXCITED POLARON STATES IN THE PROTEIN GLOBULE

Table 1 lists both electron (W) and total (I) energies and radii $\langle r\rangle$ in the excited self-consistent state (2S) and the non-self-consistent states 1S and 2P, which correspond to the potential polaron well 2S [Fig. 4(b)]. Note first that the radii of the excited self-consistent states of both two- and three-layer models, which are 19·5 and 12.2 Å, respectively, greatly exceed the mean distances between neighbouring atoms $\bar{a}$ of the medium, that is, the continuum approximation is reasonably accurate in this case. Our calculation has

shown close electron energies in the self-consistent, 2S, and non-self-consistent, 2P, states. In the three-layer case the 2P state has a higher energy level than the 2S state. Since the dipole transfer to the 1S state is possible only from the 2P state, the excited self-consistent 2S state can be expected to have a longer lifetime in the three-layer model.

Table 1 also yields an approximate estimate for the luminescence band for the three layer model, which is $\Delta W_{2P,1S} = 0.61$ eV (*ca* 2000 nm), i.e. it lies in the far-infrared range. It might be interesting to experiment with a band which being the polaron one could only be identified by a preliminary estimation of the qualitative effects that pH, ionic strength and temperature produce on the properties of the 'polaron bands.'

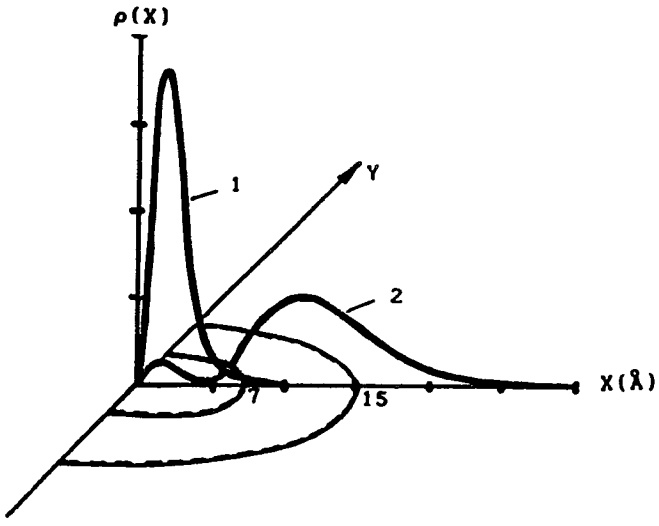

Figure 5. Distribution of electron density in the protein globule for the three-layer model; $\rho(X) = 4\pi X^2\Psi^2(X)$; 1 is the zero mode and 2 is the first mode.

THE DIELECTRIC CAVITY MODEL AND THE THEORY OF ELECTRON TRANSFER

The above considerations indicate that the electrostatic model of the protein globule is suitable for a consistent description of various processes pertaining to photoexcitation and of electron transfer processes. For example, the probability ω with which the electron of the excited self-consistent 2S state of the protein molecule can tunnel from donor to acceptor can be given by the following expression:[7,9]

$$\omega = L^2 \exp\left(-\frac{E_r}{\bar{\omega}}\right)(\pi/E_r T)^{1/2} \times \exp[-(E_r - J)^2/4E_r T] \quad (12)$$

$$E_r = 1/8\pi\tilde{\varepsilon} \int |\mathbf{D}_{2S} - \mathbf{D}_{acs}|^2 \, d\mathbf{r}$$

where L is the matrix element of tunnelling, $\mathbf{D}$ can be determined from Eqn (3), J is the reaction heat, $\bar{\omega}$ is the averaged frequency of polarization oscillations in the molecule and E_r is the total reorganization energy of the medium. Values of L and $\mathbf{D}_{acs}$ can only be determined if the acceptor model is defined.

It follows in particular from Eqn (3) that the probability of the tunnelling in the electrostatic model considered is proportional to the rate of the chemical reaction and relates to the form of the electron states by the tunnelling matrix element L and inductions $\mathbf{D}_{2S}$ and $\mathbf{D}_{acs}$. In this case of extended electron states we can expect that the constant of the reaction rate should relate to the pH of the solution and the spatial distribution of charged amino acid groups, since the induction $\mathbf{D}_{2S}[\Psi]$ of Eqn (3) depends on the polaron wave function for the most polarizable parts of the protein molecule in the layer $R_1 < r < R_2$ of our model (Fig. 5).

DISCUSSION

The introduced representations of large-radius extended states permit a completely new approach to the problem of electron transfer to large distances. The above results for the model of a dielectric cavity show that the radius of the first excited state is comparable to the size of the globule, which suggests that the whole globule is involved in the process of forming such a state. If the acceptor is near the globule and the extended self-consistent state has a similar energy to one of the acceptor's electron states, then the representation of the electron as belonging to the globule or the acceptor seperately makes no sense. If the acceptor is far from the globule, then it is significant which is the value of the tunnelling matrix element L of the electron transfer [Eqn (12)]. For a large-radius state it may be several orders of magnitude more than for a small-radius state.

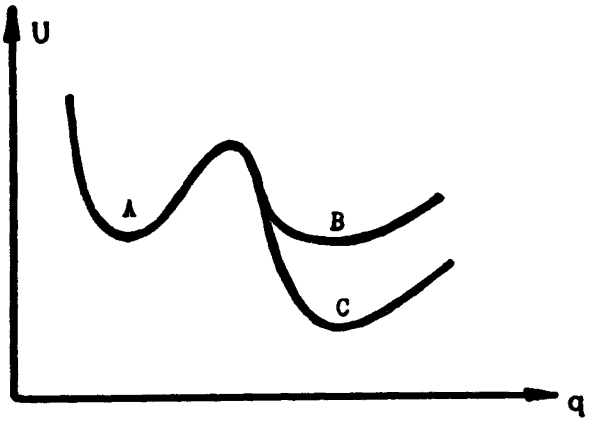

Figure 6. Simple branching of the configuration electron transfer coordinate q.

Every excited self-consistent state may be put in accordance with configuration coordinates. For a consistent description of electron transfer it is necessary to take into account that an electron can jump into intermediate self-consistent states of the acceptor and then to to the ground state. Therefore, a complex picture of electron transfer may be possible with branching of the chemical reaction coordinate (see Fig. 6). This example is a very simple case where the electron transfer from state B to state C may be both radiative and non-radiative, and in more general cases cascade radiative and non-radiative processes are possible.

The existence of excited self-consistent states may lead to interesting effects on the EPR and NMR, lines, IR absorption, etc., which can be used to identify these states. The discussion of these problems is outside of the scope of this paper, however.

APPENDIX

Finding the polaron states in the globule

1. We shall seek spherically symmetric solutions of differential Eqns (6)–(7) with boundary conditions (10) for the globule models of Figs 1 and 2. We start with passing over to new variables:

$$r = \frac{\hbar}{(2\mu|W|)^{1/2}} X;\quad \Psi(r) = \frac{|W|}{e\hbar}\left(\frac{\mu\tilde{\varepsilon}_0}{2\pi}\right)^{1/2} Y(X); \tag{A1}$$

$$\Pi(r) = \frac{|W|}{e} Z(X)$$

Normalization of the wave function yields

$$|W| = \frac{2\mu e^4}{\hbar^2}\cdot\frac{1}{\tilde{\varepsilon}_0^2\Gamma^2}$$

where

$$\Gamma = \int_0^\infty Y^2(X)X^2\,dX$$

The relationship (A1) can then be rewritten as

$$r = \frac{\hbar^2}{2\mu e^2}\tilde{\varepsilon}_0\Gamma X;$$

$$\Psi(r) = \left(\frac{2}{\pi}\right)^{1/2}\mu^{3/2}e^3\hbar^{-3}\frac{Y(X)}{\Gamma^2\tilde{\varepsilon}_0^{3/2}}; \tag{A1'}$$

$$\Pi(r) = \frac{2\mu e^3}{\hbar^2}\cdot\frac{Z(X)}{\Gamma^2\tilde{\varepsilon}_0^2}$$

We also introduce the notation $\hat{\Phi}(X)$: $\Phi(r) = (|W|/e)\hat{\Phi}(X)$.

By substituting Eqns (A1) into Eqns (6) and (7), we obtain equations with spherically symmetrical solutions:

$$\frac{d^2Y(X)}{dX^2} + \frac{2}{X}\cdot\frac{dY(X)}{dX} + Y(X)[Z(X) + \hat{\Phi}(X) - 1] = 0 \tag{A2}$$

$$\frac{d^2Z(X)}{dX^2} + \frac{2}{X}\cdot\frac{dZ(X)}{dX} + \varkappa(X)Y^2(X) = 0$$

For the protein globule (Fig. 1):

$$\hat{\Phi}(X) = \begin{cases} \dfrac{N}{X}\cdot\dfrac{\varepsilon_0}{\varepsilon_1} + \dfrac{N}{X_R}\left(1 - \dfrac{\varepsilon_0}{\varepsilon_1}\right) & X < X_R \\ \dfrac{N}{X_R} & X \geqslant X_R \end{cases}$$

where X_R is the scaled radius of the globule such that $R = (\hbar^2/2\mu e^2)\tilde{\varepsilon}_0\Gamma X_R$. The new parameter N is proportional to the charge $q = Ze$, so that

$$N = \left(\frac{2\mu}{|W|}\right)^{1/2}\frac{eq}{\hbar\varepsilon_0} = \Gamma Z\frac{\tilde{\varepsilon}_0}{\varepsilon_0}$$

The piecewise-constant function $\varkappa(X)$ breaks on the surface of the globule so that

$$\varkappa(x) = \begin{cases} \tilde{\varepsilon}_0/\tilde{\varepsilon}_1 & X < X_R \\ 1 & X \geqslant X_R \end{cases}$$

Analogously, for the three-layer model of Fig. 2:

$$\hat{\phi}(X)=\begin{cases}\dfrac{N}{X}\cdot\dfrac{\varepsilon_0}{\varepsilon_1}+\dfrac{N}{X_{R_1}}\left(\dfrac{\varepsilon_0}{\varepsilon_2}-\dfrac{\varepsilon_0}{\varepsilon_1}\right)+\dfrac{N}{X_{R_2}}\left(1-\dfrac{\varepsilon_0}{\varepsilon_2}\right) & X<X_{R_1}\\ \dfrac{N}{X}\cdot\dfrac{\varepsilon_0}{\varepsilon_2}+\dfrac{N}{X_{R_2}}\left(1-\dfrac{\varepsilon_0}{\varepsilon_2}\right) & X_{R_1}\leqslant X\leqslant X_{R_2}\\ \dfrac{N}{X} & X>X_{R_2}\end{cases}$$

$$\varkappa(X)=\begin{cases}\tilde{\varepsilon}_0/\tilde{\varepsilon}_0 & X<X_{R_1}\\ \tilde{\varepsilon}_0/\tilde{\varepsilon}_2 & X_{R_1}\leqslant X<X_{R_2}\\ 1 & X\geqslant X_{R_2}\end{cases}$$

The solution of Eqns (A2) should satisfy the infinity conditions following from Eqn (10), be finite at zero and meet the corresponding internal boundary conditions at points of breaks in the piecewise-constant function $\varkappa(X)$.

The boundary solutions for Eqns (A2) have the form

$$2Y'(0)+N\frac{\varepsilon_0}{\varepsilon_1}Y(0)=Y(\infty)=0,\qquad Z'(0)=Z(\infty)=0 \tag{A3}$$

For the internal boundary conditions:

$$\begin{aligned}Y(X_{R_i}-0)&=Y(X_{R_i}+0),\\ Y'(X_{R_i}-0)&=Y'(X_{R_i}+0)\\ Z(X_{R_i}-0)&=Z(X_{R_i}+0),\\ \tilde{\varepsilon}_iZ'(X_{R_i}-0)&=\tilde{\varepsilon}_{i+1}Z'(X_{R_i}+0)\end{aligned} \tag{A3'}$$

Here $i=1$ for the two-layer globule ($R_1=R$, $\tilde{\varepsilon}_2=\tilde{\varepsilon}_0$) and $i=1$, 2 for the three-layer globule ($\tilde{\varepsilon}_3\equiv\tilde{\varepsilon}_0$).

2. The solutions of the problem (A2) with boundary conditions (A3) and internal boundary conditions (A3′) were found in the same way as the solutions of the polaron problem in a homogeneous polar medium[12] and of the F-centre problem.[13]

The procedure for finding solutions is obvious for the polaron problem in a homogeneous polar medium, so we shall take this case to describe the algorithm. Then, as we have already mentioned, we shall pass over to the problems which are our immediate interest.

2.1. The equations of the polaron in a homogeneous medium can be regarded as the particular case of Eqns (A2) where $\varepsilon_i=\varepsilon_0$ and $N=0$. The mathematical formulation reduces to finding the solutions of the boundary-valued problem:

$$\begin{aligned}Y''(X)+\frac{2}{X}\cdot Y'(X)+Z(X)Y(X)-Y(X)&=0\\ Z''(x)+\frac{2}{X}\cdot Z'(X)+Y^2(X)&=0\\ Y'(0)=Z'(0)=0;\ Y(\infty)=Z(\infty)&=0\end{aligned} \tag{A4}$$

It was shown[12] that this problem has a number of solutions in which $Z_n(X)$ ($n=0,1,2,\ldots$) monotonically tends to zero as $X\to 0$, and $Y_n(X)$ crosses the axis X n times, after which it tends to zero as $X\to\infty$.

Now we change variables so that

$$\zeta=XY,\qquad \eta=XZ$$

and Eqns (A4) assume the form

$$\begin{aligned}\zeta''+\zeta(\eta/X-1)&=0\\ \eta''+\zeta^2/X&=0\end{aligned} \tag{A5}$$

$$\zeta(0)=\eta(0)=0;\ \zeta(\infty)=\eta'(\infty)=0 \tag{A6}$$

2.2. The solutions of Eqns (A5), which only satisfy the left-hand boundary condition of Eqns (A6) in the neighbourhood of the point $X=0$, may be represented as power series:

$$\begin{aligned}\zeta(x)&=a_1X+a_2X^2+a_3X^3+\cdots\\ \eta(X)&=b_1X+b_2X^2+b_3X^3+\cdots\end{aligned}$$

If we substitute these series into Eqns (A5), we can see that all coefficients a_i and b_i are expressed in terms of $a_1\equiv a$ and $b_1\equiv b$. Confining ourselves to the first few terms of the series, we can, at a point X_0 which is not distant from $X=0$, find a desirably accurate values of $\zeta(X_0;a,b)$ and $\eta(X_0;a,b)$ and their derivatives corresponding to definite values of parameters a and b.

2.3. For the system of differential equations (A5) we define the Cauchy problem in the interval $[X_0,X_k]$. To this end, for $X=X_0$ (X_0 is small), we determine $\zeta(X_0;a,b)$ and $\eta(X_0;a,b)$, $\eta'(X_0;a,b)$ at prescribed values of a and b. Then the solution is found numerically on a computer by the standard Runge–Kutta method.

Note that the second equation of Eqns (A5) yields a convex function $\eta(X)$, so that $\eta''(X)<0$ for all $X\geqslant 0$. This property of $\eta(X)$ is central in finding the solution of a boundary-value problem. If we succeed in choosing the values of a and b such that $\eta(X)$ tends to a constant as $X\to\infty$,

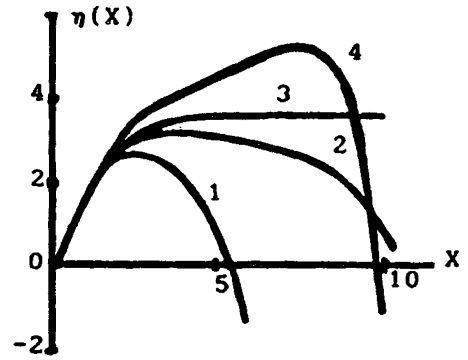

Figure 7. Functions $\eta(X)$ for various initial data given by a and b: (1) $a = 1.2$, $b = 2.0$; (2) $a = 1.1$, $b = 2.0$; (3) $a = 1.02$, $b = 1.94$; (4) $a = 1.0$, $b = 2.0$.

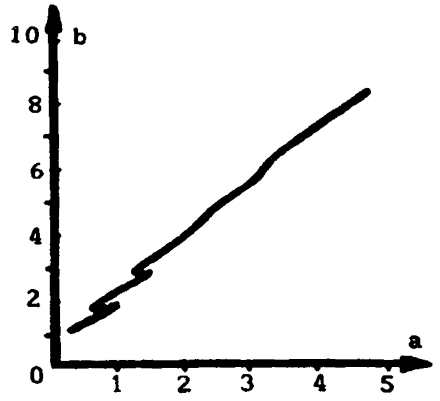

Figure 8. Dependence between a and b following from Eqn (A7) at $X = 10$.

then $\zeta(X)$ will tend to zero. This would mean a solution of the boundary-value problem of Eqns (A5) and (A6) is found.

2.4. We now choose the values of parameters a and b and solve within an interval $[X_0, X_K]$ the emerging Cauchy problems. Figure 7 shows some of such solutions. Take an X_K which corresponds to the maximum of one of them, such that $a = a^*$ and $b = b^*$ (a^* and b^* are definite numbers). Define a function

$$F(a, b) \equiv \eta'(X_K; a, b)$$

Let us now take the Cauchy problem for a new interval $[X_0, X_K]$, which, when solved for some a and b, will yield the values of the function $F(a, b)$. The equation

$$F(a, b) = 0 \qquad \text{(A7)}$$

is an implicit dependence between a and b. Here, the choice of X_K determines one of the points of this dependence which is $F(a^*, b^*) = 0$.

The dependence (A7) in the prescribed intervals of a and b may be found with the CURVE program complex.[22] Figure 8 shows a curve which was obtained with this program.

The solutions of the Cauchy problem for a and b along the curve can be seen in Fig. 9. An analysis of the curves $\zeta(X)$ suggests the existence of a series of solutions of the boundary-value problem in Eqns (A5) and (A6). They may be arranged as follows: $\zeta_n(X)$, with $n = 0,1,2,\ldots$, crosses the axis X, n times, after which it exponentially tends to zero; and $\eta_n(X)$ grows monotonically to its extreme value $\eta_n(\infty)$.

2.5. We define a system of two functions of three variables:

$$F_1(a, b, X_K) \equiv \zeta'(X_K; a, b)$$
$$F_2(a, b, X_K) \equiv \eta'(X_K; a, b) \qquad \text{(A8)}$$

This definition means that for the values of F_1 and F_2 to be determined, the Cauchy problem should be solved in the interval $[X_0, X_K]$ with the initial values corresponding to those of parameters a and b. The values of ζ' and η' in the end of the integration path give the values of the functions. The system of equations

$$F_1(a, b, X_K) = 0$$
$$F_2(a, b, X_K) = 0 \qquad \text{(A9)}$$

locates a curve in the space of variables a, b and X_K. We determined pieces of several branches of the curve. To this end, we chose initial approximations to each branch from the calculations above, then ran the program CURVE to find points of the curve (A9) which correspond to the values of the variables a, b and X_K in the prescribed range.

As $X_K \to \infty$, the conditions (A9) are identical with the right-hand boundary conditions (A6). Actually, in polaron problem we only had to go up to $X_K = 10$ for the zero mode ($n = 0$), $X_K = 15$ for the first mode ($n = 1$) and $X_k = 20$ for the second mode ($n = 2$) to obtain the solutions of the boundary-valued problem in Eqns (A5) and (A6) with a given accuracy.

Figure 10 shows two of the solutions obtained by this procedure.

3. The F-centre problem differs from the polaron problem for a homogeneous polar medium by additional terms NY/X in the first of Eqns (A3), where N is the problem's parameter.

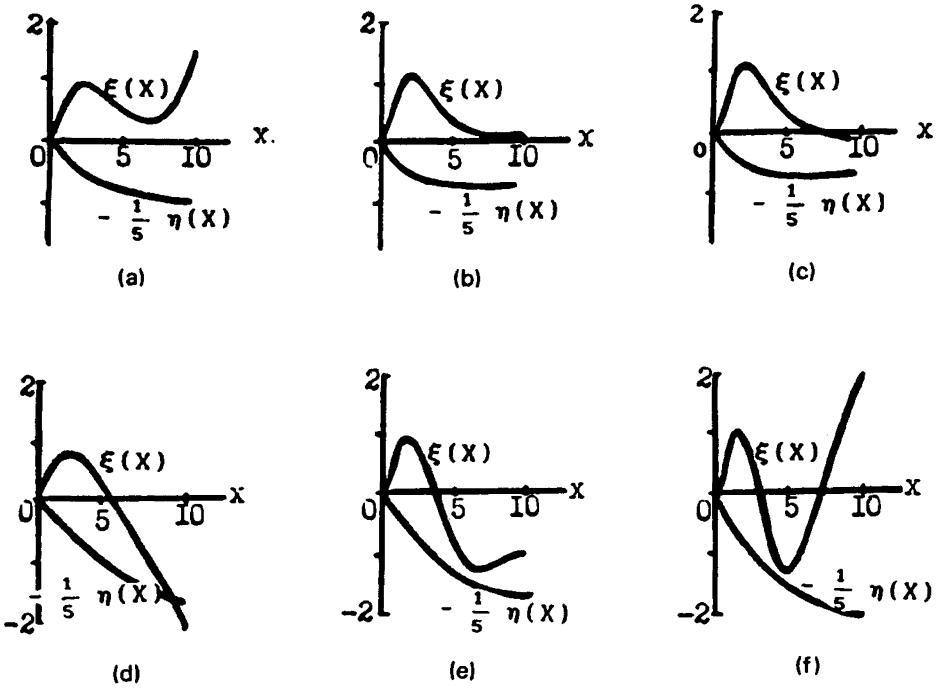

Figure 9. Solutions of the Cauchy problem for various a and b on the curve (A9) of Fig. 8:(a) $a = 0.733$, $b = 1.664$; (b) $a = 1.003$, $b = 1.921$; (c) $a = 1.025$, $b = 1.942$; (d) $a = 0.623$, $b = 1.662$; (e) $a = 0.900$, $b = 2.074$; (f) $a = 1.338$, $b = 2.727$.

We sought solutions for various N on the curves which pass through the polaron solutions. The system of equations is

$$F_1(N, a, b) \equiv \zeta'(X_K; N, a, b) = 0$$
$$F_2(N, a, b) \equiv \eta'(X_K; N, a, b) = 0 \qquad \text{(A10)}$$

The curve (A10) started from the known values at $N = 0$ for the polaron states. The actual dependences were found by the CURVE program. To refine the solution for a given N we introduced new functions:

$$F_1(a, b, X_K) \equiv \zeta'(X_K; N, a, b)$$
$$F_2(a, b, X_K) \equiv \eta'(X_K; N, a, b)$$

and proceeded as for the polaron case for system (A9).

4. The above polaron and F-centre problems help to find spherically symmetrically polaron states in various models of the protein globule. Let us consider the two-layer model of Fig. 1, for which the case of many-layer models differs merely in technical details.

The initial model [Eqns (6) and (7)] takes as physical parameters the values $\{\varepsilon_1, \varepsilon_2, \varepsilon_\infty, R, Z\}$. The boundary-valued problem in Eqns (A2) and (A3) contains X_R and N, instead of R and Z,

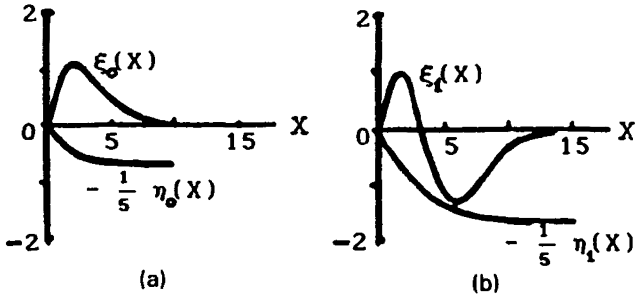

Figure 10. Solutions of the boundary-value problem in Eqns (A5) and (A6): (a) $a = 1.021$, $b = 1.938$; (b) $a = 1.091$, $b = 2.320$.

which are interrelated as

$$X_R = R \cdot \frac{2\mu e^2}{\tilde{\varepsilon}_0 \hbar^2} \cdot \Gamma^{-1}, \qquad N = Z \cdot \frac{\tilde{\varepsilon}_0}{\varepsilon_0} \cdot \Gamma \qquad \text{(A11)}$$

Since the value of $\Gamma = \int_0^\infty Y^2(X) X^2 \, dX$ is not known beforehand, the values of X_R and N, which appear in the equations and correspond to a preset globule radius R and charge Z, are not known. The only parameter known is their product:

$$NX_R = \frac{2\mu e^2}{\hbar^2} \cdot \frac{RZ}{\varepsilon_0} = \text{constant} \qquad \text{(A12)}$$

The right-hand side of Eqn (A12) contains universal constants and model parameters only. The dependence (A12) suggests the following algorithm for finding the solutions, as follows.

1st step. We change variables as $\zeta = YX$ and $\eta = ZX$. Then, representing $\zeta(X)$ and $\eta(X)$ as power series:

$$\zeta(X) = a_1X + a_2X^2 + \cdots$$
$$\eta(X) = b_1X + b_2X^2 + \ldots$$

and substituting them in (A2) we find a two-parameter family of solutions of differential equations (A2) in the neighbourhood of the point $X = 0$ which satisfy the left-hand boundary condition (A3). Parameters a and b are equal to $Y(0) = Y_0$ and $Z(0) = Z_0$, respectively.

2nd step. We start from the known solutions for the F-centre. Let T_0^*, Z_0^* and N^* be the values of medium parameters which determine a mode of the F-centre. Then, from Eqn (A12), $X_K^* = \text{constant}/N^*$. The system of equations is defined as

$$\begin{aligned} F_1(Y_0, Z_0, \varepsilon_1) &\equiv \zeta'(X_K; Y_0, Z_0, \varepsilon_1) = 0 \\ F_2(Y_0, Z_0, \varepsilon_1) &\equiv \eta'(X_K; Y_0, Z_0, \varepsilon_1) = 0 \end{aligned} \quad \text{(A13)}$$

Put $\varepsilon_1 = 80$ and $N = N^*$. Then the point $(Y_0, Z_0, \varepsilon_1) = (Y_0^*, Z_0^*, \varepsilon_0)$ will belong to the curve (A13), because of the initial values of parameters. We may make use of the CURVE program to locate the branch of the curve which passes through this point. Therefore, we can go from $\varepsilon_1 = 80$ to $\varepsilon_1 = 20$ which was prescribed to the two-layer model.

3rd step. The system of equations is

$$\begin{aligned} G_1(Y_0, Z_0, N) &\equiv \zeta'(X_K; Y_0, Z_0, N) = 0 \\ G_2(Y_0, Z_0, N) &\equiv \eta'(X_K; Y_0, Z_0, N) = 0 \end{aligned} \quad \text{(A14)}$$

Starting from the previous solution at $\varepsilon_0 = 80$, $\varepsilon_1 = 20$ and appropriate parameter values of Y_0, Z_0 and N, we locate the branch of the curve (A14) by the CURVE program. Then we calculate $\Gamma = \int_0^\infty Y^2X^2\,dX$, at each of the found points of the curve, and put

$$R = X_R\Gamma \cdot \frac{\hbar e^2}{2\mu e^2} \quad \text{and} \quad Z = \frac{N}{\Gamma} \cdot \frac{\tilde{\varepsilon}_0}{\varepsilon_0}$$

We can move along the curve until we reach the parameters $R = 15$ Å and $Z = 1$ [from Eqn (A12) these values will emerge one at a time]. In this way, we can find a solution to this case of the boundary-value problem.

4th step. If desired, the solution may be refined: X_K should become the parameter and should move towards larger values. Examples of solutions for the globule's polaron states are shown in Fig. 4,

5. The spectral electron's characteristics in the potential field of self-consistent polaron states were found by solving the linear Schrödinger equation with potential $U(X) = Z_n(X) + \hat{\Phi}(X)$, where $Z_n(X)$ is the nth solution of the boundary-value problem in Eqns (A2) and (A3). However, there are some limitations caused by the function $Z_n(X)$ defined for a discrete sequence of non-uniformly spaced points only. It is common practice to use interpolation equations here. However, we proceeded in a different way and appended the linear Schrödinger equation:

$$\chi'' - \frac{l(l+1)}{X^2}\chi + \chi\left(\frac{\eta}{X} + \hat{\Phi}\right) - \lambda\chi = 0 \quad \text{(A15)}$$

by the following equations for polaron states:

$$\begin{aligned} \zeta'' + \zeta(\eta/X + \hat{\Phi}) - \zeta &= 0 \\ \eta'' + \varkappa(X)\zeta^2/X &= 0 \end{aligned} \quad \text{(A16)}$$

and combined the three into a single system of differential equations. The variable χ is absent in Eqns (A16), and therefore $\eta(X)$ of Eqn (A15) emerges every time in the same form, which also corresponds to the polaron mode at points conforming to Eqn (A15) and is independent of the values and initial data for $\chi(X)$. At given l (orbital moment) and n (number of zeroes), λ was found by the half-division procedure. The results are given in Table 1.

Acknowledgements

The authors are grateful to L. V. Lunevskaya and O. M. Liginchenko for their help in preparing the manuscript.

REFERENCES

1. D. De Vault and B. Chance, *Biophys. J.* **6**, 825 (1966).
2. B. Chance (Ed.), *Tunnelling in Biological Systems*. Academic Press, New York (1979).
3. R. A. Marcus and N. Sutin, *Biochim. Biophys. Acta* **811** 265 (1985).
4. T. Foerster, *Naturwissenchaften* **33**, 166 (1946).

5. T. Foerster, *Discuss. Faraday Soc.* **27**, 7 (1959).
6. R. A. Marcus, *Annu. Rev. Phys. Chem.* **15**, 155 (1964).
7. J. Jortner, *J. Chem. Phys.* **64**, 4860 (1976).
8. J. J. Hopfield, *Proc. Natl. Acad. Sci. USA*, 3640 (1974).
9. J. J. Hopfield, *Biophys. J.* **18**, 311 (1977).
10. S. Pekar, *Untersuchungen über die Electronentheorie der Kristalle*. Academie-Verlag, Berlin (1954).
11. K. Huang and A. Rhys, *Proc. R. Soc. London* **204**, 406 (1950).
12. N. K. Balabaev and V. D. Lakhno, *Teor. Mat. Fiz.* **45**, 139 (1980).
13. V. D. Lakhno and N. K. Balabaev, *Opt. Spektrosc.* **55**, 308 (1983).
14. S. E. Bresler and D. L. Talmud, *Dokl. Akad. Nauk SSSR* **43**, 326 (1944).
15. C. Tenford and J. G. Kirkwood, *J. Am. Chem. Soc.* **79**, 5333 (1957).
16. J. B. Mattew, *Annu. Rev. Biophys. Chem.* **14**, 387 (1985).
17. C. Tenford, *Physical Chemistry of Macromolecules*. Wiley, New York (1961).
18. K. Rogers, *Prog. Biophys. Mol. Biol.* **48**, 37 (1986).
19. A. A. Kornyshev, R. Dogonadze and J. Ulsirup, in *The Chemical Physics of Solvation, Part A*, p. 70. Elsevier, Amsterdam (1985), R. Dogonadze *et al.*, eds.
20. T. Spiro, (Ed.) *Copper Proteins*. Wiley, New York (1981).
21. P. Morrison, (Ed.) *Metalloproteins, Part 1*. Macmillan, London (1985).
22. N. K. Balabaev and L. V. Lunevskaya, *Motion Along a Curve in n-Dimensional Space. FORTRAN, Algorithms and Programs*. SSSR, *Akademiya Nauk* Puchchino (1978).